MHD stability analysis and studies of Alfvénic modes with energetic particles in DTT

V.Fusco[1], G. Vlad[2], S. Mastrostefano[1], M. V. Falessi[1], F. Zonca[1,3], S. Briguglio[4], E. Giovannozzi[1], I. Casiraghi[5], C. De Piccoli[4], Q. Hu[5,7], P. Mantica[5], P. Vincenzi[4,6]

[1]*ENEA, C. R. Frascati, Via E. Fermi 45, 00044 Frascati (Roma), Italy*

[2] *Consorzio CREATE, via Claudio 21, 80125 Napoli (Italy)*

[3]*Institute for Fusion Theory and Simulation and Department of Physics, Zhejiang University, Hangzhou 310027, China*

[4]*Consorzio RFX (CNR, ENEA, INFN, Università di Padova, Acciaierie Venete SpA), Corso Stati Uniti 4, 35127 Padova, Italy*

[5]*Institute for Plasma Science and Technology, CNR, Milano, Italy*

[6]*Institute for Plasma Science and Technology, CNR, Padova, Italy*

[7]*Dipartimento di Fisica 'G. Occhialini', Università di Milano-Bicocca, Milano, Italy*

Abstract We present a systematic linear MHD and hybrid MHD-kinetic analysis of Alfvénic modes driven by energetic ions in the Single Null, positive-triangularity, full-power DTT scenario. Using coupled equilibrium (CHEASE), resistive MHD (MARS), continuum (FALCON) and hybrid MHD-gyrokinetic (HYMAGYC) codes, we characterise internal kink, infernal, TAE and EPM stability and quantify growth rates and localization for a realistic slowing-down fast-ion distribution. We find distinct EPM and TAE branches with different radial localization and growth-rate scalings; EPMs dominate at low-n while TAEs are unstable across moderate–high n.

Introduction The Divertor Tokamak Test (DTT) facility represents a crucial step in the European fusion roadmap. A rigorous characterisation of its MHD stability, Alfvénic spectrum, and energetic-particle dynamics is both scientifically relevant and operationally essential. MHD instabilities, from large-scale disruptions to localized internal modes, can degrade confinement and damage plasma-facing components, making stability assessment indispensable for defining safe operational boundaries.

Alfvénic eigenmodes (e.g., TAEs, EAEs) occur in frequency gaps of the Alfvén continuum. Energetic particles, produced by NBI/ICRH or born as fusion alphas, have velocities comparable to the Alfvén velocity and can resonantly drive Alfvénic eigenmodes and energetic-particle modes (EPMs). When unstable, these modes can induce fast-ion radial transport, inhibit thermalization, reduce heating efficiency, and potentially damage the first wall. This work reports a linear, drift-kinetic, collisionless study of DTT reference scenarios: we characterise MHD stability, compute the Alfvén continuum/gap structure, and investigate linear energetic-particle-driven instabilities using a fitted slowing-down distribution derived from ASCOT.

Numerical Simulations Approach The study adopts a global, kinetic, self-consistent approach retaining realistic equilibrium geometry, plasma non-uniformities. Collisions are

neglected; finite-orbit-width (drift-kinetic) effects are retained while full FLR physics is not. Only linear evolution is considered here. The code workflow consists of: CHEASE (Grad–Shafranov equilibria with high resolution [2]); MARS (global resistive MHD eigenvalue code for continuum structure and discrete eigenmode identification without energetic particles [3]); HYMAGYC (hybrid MHD–gyrokinetic initial-value code for self-consistent linear (and future nonlinear) evolution with energetic particles [4]); FALCON (computes the Alfvén continuum and gap structure for realistic geometries [5]).

Equilibria and Input Data The analysis focuses on the Single Null (SN), positive-triangularity, full-power DTT scenario. Three scenarios are considered (green, black, red in Fig. 1) [6-7]; the red one, shot 3838, is the most recent and includes an empirical sawtooth model. All share an extended $q < 1$ region and low core magnetic shear. The green and black equilibria have steep core pressure gradients; the red equilibrium shows a flattened core pressure due to sawtooth redistribution, with favourable consequences for infernal mode stability.

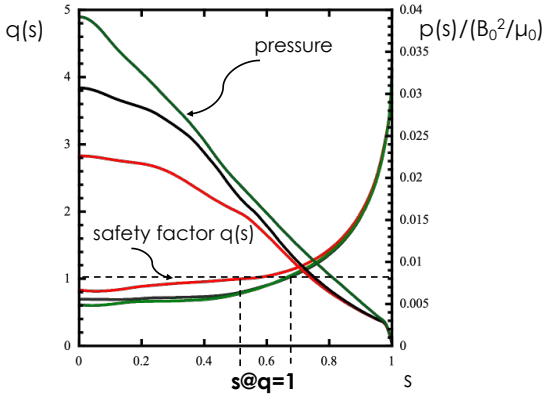

Figure 1: Equilibria for different shots. Pressure p (r.h.s) and safety factor q (l.h.s.) are represented.

The multi-species mass density $\rho(s) = \Sigma_i m_i n_i$ governs the MHD equations and the Alfvén velocity (s is the normalized radial-like coordinate); in this contest, the plasma species are D, Ar, and W. A density-weighted mean atomic mass $\langle A \rangle = \Sigma_i A_i Z_i n_i(0)/n_e(0)$ defines an effective mean on-axis ion density $\langle n_i(0) \rangle = \rho/(\langle A \rangle u)$, where u is the unit mass density, and n_e is the electron density.

The fast-ion density profile has been obtained from an ASCOT simulation [8] and peaks off-axis at $n_{Hpeak} = 1.8\times10^{18}$ m^{-3} ($n_{H0} = 6.3\times10^{17}$ m^{-3}). While the present work covers multiple DTT equilibrium scenarios, ASCOT calculations of the fast-particle distribution function were performed on a single magnetic equilibrium and kinetic profiles representative of the scenarios analyzed and considering only NBI heating. The distribution function used in HYMAGYC to approximate the numerical results is: $\hat{F}_0 = \hat{f}_{sd}(E, s)\ \Theta(\alpha, \alpha_0, \Delta)$ with slowing-down energy dependence ($E_0 = 510$ keV, the injection energy and $E_{c0} = 213.6$ keV the critical energy) and Gaussian pitch-angle anisotropy ($\alpha_0 = -27°$, $\Delta = 0.466$) (see [9] for slowing-down and Θ definition), fitted to ASCOT output [10]. The fitting has been obtained comparing the theoretical distribution function over three parameters: the normalized radius (s), pitch angle (α), and energy (E) and comparing it with ASCOT to find a best fit over the parameter Δ that represents the anisotropy width.

MHD Stability *Internal kink and sawtooth.* All equilibria show a q=1 surface inside the plasma thus being internal kink unstable. The large $q < 1$ region raises some concern for severe sawtooth crashes with core confinement impact and eventually Neoclassical Tearing Mode (NTM) seeding; anyway, note that the scenario simulated including the sawtooth model (shot 3838) reduces the $q = 1$ radius and q_0 excursion, mitigating the drive. ECRH/ECCD are identified as a complementary control tool for q-profile tailoring.

Infernal modes. The combination of low shear and steep core pressure gradients in the green and black equilibria drives a large variety of infernal modes — low-n pressure-driven internal instabilities identified by Manickam et al. [11]. Their growth rate is an oscillatory function of n (not monotonically decreasing as standard ballooning theory predicts), making stability predictions sensitive to the precise q_0 value. Nonlinearly, infernal modes can seed NTMs, as documented on JET [12], and may develop extended radial structures enhancing core transport [13]. DTT-specific results are reported in [14-15]. On the contrary, shot 3838 (red curve in Fig.1) does not exhibit infernal modes: the sawtooth-induced pressure flattening removes the drive. This suppression is however transient, as profiles rebuild between crashes, infernal mode conditions may periodically re-emerge across the sawtooth cycle and it will be checked in the near future. This suppression is however transient, as profiles rebuild between crashes and infernal mode conditions may periodically re-emerge across the sawtooth cycle; this will be checked in the near future.

TAE stability (MARS). Eigenmode spectrum of TAEs lies within the continuum gap; in the absence of fast ions all modes are damped ($\gamma < 0$) via continuum damping, whose magnitude correlates with eigenfunction overlap at the gap edges. This establishes the damping baseline that fast-ion drive must overcome.

Energetic Particles Driven Instabilities: HYMAGYC Analysis

Numerical setup. A simulation scan n = 2–30 has been carried out. Poloidal harmonic number, radial s-mesh, and χ-mesh have been validated by convergence tests; indeed high-n cases require finer grids. Moreover, we consider plasma boundary truncation (e.g. $q_{92\%}$) that reduces numerical resources required to correctly resolve the full original plasma domain.

Results. Two distinct unstable branches are identified across the n scan (Figs. 2): Energetic Particle Modes (EPMs, red squares) and Toroidal Alfvén Eigenmodes (TAEs, blue circles). It's worth noting that $n_H(s)$ peaks near $s \simeq 0.25$ and two large drive ($\partial n_H/\partial s$) regions coexist: a positive gradient ($\partial n_H/\partial s > 0$) inward of the peak, and a negative gradient ($\partial n_H/\partial s < 0$) on the outer slope. The EPMs is radially localized close to axis, near $s \simeq 0.1$, where the gradient is positive ($\partial n_H/\partial s > 0$) and the TAE is localised near $s \simeq 0.4$ where the gradient is negative ($\partial n_H/\partial s < 0$), on the outer slope. This spatial separation and frequency sign, which is opposite to one another, is directly visible in Fig. 3 and constitutes a direct confirmation of the gradient-drive

picture.

The EPM branch appears at low toroidal mode numbers (n = 2, 4, 10) with growth rates significantly exceeding those of TAEs, reaching $\gamma/\omega_{A0} \simeq 0.015$ at n = 2 and decreasing with n.

The TAE branch is unstable across the full range n = 8–30, with $\gamma/\omega_{A0} \simeq 0.003$–$0.005$ varying modestly and non-monotonically with n, where the on-axis Alfvén angular frequency is $\omega_{A0}=2.7\text{x}10^6$rad/s; the n = 2 TAE is stable, indicating that continuum damping exceeds the energetic particle drive at the lowest toroidal mode numbers.

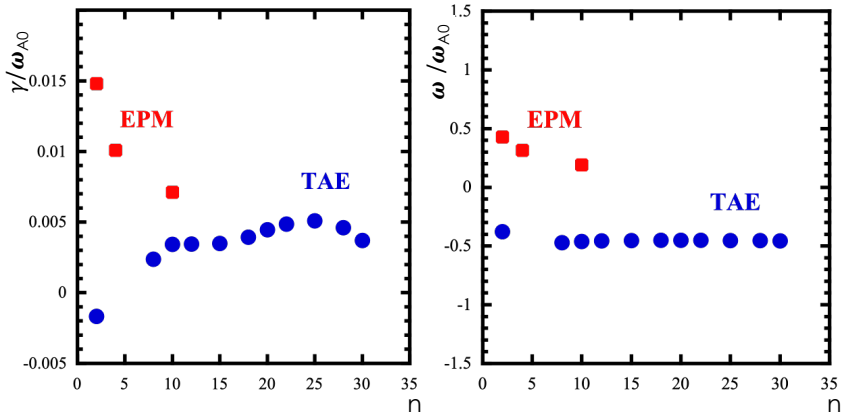

Figure 2: Energetic Particle Modes (EPMs, red squares) and Toroidal Alfvén Eigenmodes (TAEs, blue circles), growth rates (l.h.s) and angular frequency (r.h.s)

TAE frequencies lie within the continuum gap with little n-dependence; EPM frequencies, unconstrained by the gap, track the fast-ion resonance conditions. These global, model slowing down distribution results extend the local analysis of [16] and the Maxwellian study of [1].

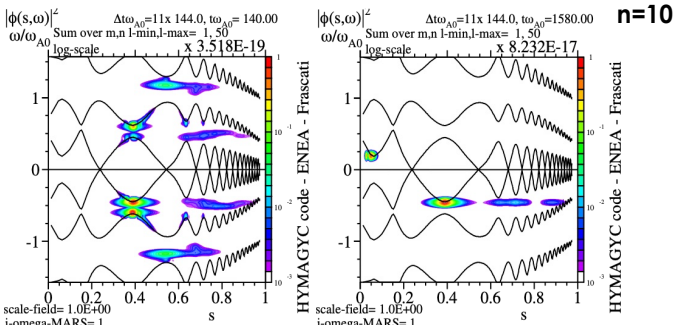

Figure 3: Frequency Spectra of the electrostatic potential $\phi(s,\omega)$ for n=10 at different time

The temporal evolution of the power spectra of the scalar potential $|\phi(s,\omega)|^2$ and of the total energy depicts both the mode identification and the nonlinear saturation. In Fig.3, for n = 10 as an example, the evolution is qualitatively rich: at $t\omega_{A0} = 140$ spectral power concentrates near the TAE gap frequency at mid-radius; by $t\omega_{A0} = 1580$ a second discrete feature appears near $s \simeq 0.1$ at the EPM frequency, revealing sequential excitation, TAE first, EPM later. The detailed characterisation of the saturation physics is deferred to future nonlinear work.

References

[1] G. Giruzzi et al 2026 Nucl. Fusion in press https://doi.org/10.1088/1741-4326/ae7a8d; [2] H. Lütjens et al., Comput. Phys. Commun. 97 (1996) 219–260; [3] A. Bondeson et al., Phys. Fluids B 4 (1992) 1889–1900; [4] G. Vlad et al, 2025 Reviews of Modern Plasma Physics 9:27 https://doi.org/10.1007/s41614-025-00199-2; [5] M. V. Falessi et al. 2020 Jour. Plasma Phys. **86** 845860501; [6] I. Casiraghi et al., Plasma Phys. Control. Fusion 65 (2023) 035017; [7] P. Mantica et al., Conferenza Italiana Plasmi (2026); [8] E. Hirvijoki et al, 2014 Comp. Phys. Comm. **185** 1310; [9] G. Vlad et al., Nucl. Fusion 49 075024 (2009); [10] C.De Piccoli et al., Front. Phys. 12 (2024) 1492095; [11] J. Manickam et al., Nucl. Fusion 27 (1987); [12] D. Brunetti et al., J. Phys.: Conf. Ser. 775 012002 (2016); [13] M. Coste-Sarguet et al., Plasma Phys. Control. Fusion 66 (2024); [14] V.Fusco et al., EPS 2022, P2a.125. (2022); [15] F. Crisanti et al., Nucl. Fusion 64, 106040 (2024); [16] G. Wei et al., 2026 Plasma Phys. Control. Fusion 68 045021